J|A|C|S
ARTICLES
Published on Web 04/18/2006

A Thermodynamically Stable Nanophase Material

Zhang Lin,[†] Benjamin Gilbert,[‡] Quanlin Liu,[§] Guoqiang Ren,[†] and Feng Huang*,[†]

Contribution from the Laboratory of Materials Chemistry and Physics, Fujian Institute of Research on the Structure of Matter, National Engineering Research Center for Optoelectronic Crystalline Materials, Chinese Academy of Sciences, Fuzhou, Fujian, 350002, People's Republic of China, Earth Sciences Division, Lawrence Berkeley National Laboratory, Berkeley, California 94720, and Department of Materials Physics and Chemistry, University of Science and Technology Beijing, Beijing 100083, People's Republic of China

Received October 27, 2005; E-mail: fhuang@fjirsm.ac.cn

Abstract: Nanoparticles are metastable relative to the equivalent bulk material due to the positive excess interfacial free energy (IFE). Previous studies have shown that, with increasing surface interaction strength, the IFE diminishes but remains positive. We describe an experimental multicomponent system in which a nanoscale ZnS material is thermodynamically favored and can be formed at the expense of bulk ZnS. In 17 M sodium hydroxide solution, at 230 °C, both 3 nm ZnS nanoparticles and bulk ZnS are transformed into sheetlike nanocrystals with a ZnS polytype structure. Our results are theoretically compatible with the concept of a negative IFE, although not with the assumption of constant interface composition. We clarify the meaning of an effective negative IFE and present the necessary conditions for strong chemical surface interactions to stabilize nanoscale inorganic materials relative to bulk matter. Our results show that synthesis methods employing thermodynamic controls can produce nanomaterials with novel morphology.

Introduction

The synthesis of nanoparticles with a single size and morphology is one of the most significant challenges in nanotechnology.[1−3] The difficulty arises because nanoparticles are normally metastable relative to the equivalent bulk material.[4−7] Due to the thermodynamic tendency for growth, a finite size distribution of metastable nanoparticles cannot be avoided without sophisticated controls on growth kinetics. In general chemical syntheses, capping ligands are introduced to "arrest" growth and thus limit particle size.[8] A desirable alternative strategy would be to realize an equilibrium system in which a nanophase with a certain size is thermodynamically stable, so that precursors with other sizes (including bulk) will transform into this nanophase spontaneously.

The concept of a thermodynamically stable inorganic nanophase material is well-known in materials and colloid science but remains poorly defined and lacks convincing experimental evidence. The central premise is that strongly adsorbing species can stabilize high energy termination surfaces of nanoscale particles. However, as discussed in more detail below, the stabilization of nanoparticles relative to bulk materials requires both the introduction of a formally negative interfacial free energy (IFE) term[9] and a destabilizing free energy contribution that is greater for smaller dimensions and which prevents complete dissolution. Such systems have been long realized with liquid−liquid colloids (microemulsions). However, the situation is more complex with solid−liquid colloids (nanoparticle suspensions), because interactions at the surfaces of nanocrystallites can involve strong chemical bonding and compositional changes, and both the surfaces and the interaction on them are generally anisotropic.

Although modern nanoparticle synthesis methods commonly involve strongly coordinating ligands that both modify precursor reactivity and coat the surface of the growing nanoparticle to achieve highly monodisperse size distributions, such syntheses are usually under kinetic and not thermodynamic control. Several investigators have speculated that nanoparticle stability may be thermodynamically enhanced by strongly adsorbing surface species.[10−12] Furthermore, reactive ligands can narrow the size distribution of Au[13] and PbS[14] nanoparticles and switch Co

[†] Chinese Academy of Sciences.
[‡] Lawrence Berkeley National Laboratory.
[§] University of Science and Technology Beijing.

(1) Colvin, V. L.; Schlamp, M. C.; Alivisatos, A. P. *Nature* **1994**, *370*, 354.
(2) Dabbousi, B. O.; Rodriguez Viejo, J.; Mikulec, F. V.; Heine, J. R.; Mattoussi, H.; Ober, R.; Jensen, K. F.; Bawendi, M. G. *J. Phys. Chem. B* **1997**, *101*, 9463.
(3) Teranishi, T.; Miyake, M. *Chem. Mater.* **1998**, *10*, 594.
(4) Somorjai, G. A. *Introduction to Surface Chemistry and Catalysis*; Wiley: New York, 1994.
(5) Lyklema, J. *Fundamentals of Interface and Colloid Science. Volume I: Fundamentals*; Academic Press: London, 1991.
(6) Zhang, H.; Banfield, J. F. *J. Mater. Chem.* **1998**, *8*, 2073.
(7) McHale, J. M.; Auroux, A.; Perotta, A. J.; Navrotsky, A. *Science* **1997**, *277*, 788.
(8) Cushing, B. L.; Kolesnichenko, V. L.; O'Connor, C. J. *Chem. Rev.* **2004**, *104*, 3893.
(9) Lodziana, Z.; Topsoe, N. Y.; Norskov, J. K. *Nature Materials* **2004**, *3*, 289 2004.
(10) Leff, D. V.; Ohara, P. C.; Heath, J. R.; Gelbart, W. M. *J. Phys. Chem. B* **1995**, *99*, 7036.
(11) Vayssieres, L.; Chaneac, C.; Tronc, E.; Jolivet, J. P. *J. Colloid Interface Sci.* **1998**, *205*, 205.
(12) Mladenovic, I. L.; Kegel, W. K.; Bomans, P.; Frederik, P. M. *J. Phys. Chem. B* **2003**, *107*, 5717.
(13) Stoeva, S.; Klabunde, K. J.; Sorensen, C. M.; Dragieva, I. *J. Am. Chem. Soc.* **2002**, *124*, 2305.
(14) Hines, M. A.; Scholes, G. D. *Adv. Mater.* **2003**, *15*, 1844.

10.1021/ja057121p CCC: $33.50

between nanocrystal and cluster complex states[15] through a process termed "digestive ripening". Moreover, both kinetic and thermodynamic controls on the size and shape of semiconducting nanoparticles have been identified in high-resolution TEM studies of nanoparticles synthesized under varying conditions.[16,17] These results are suggestive of a free energy driving force for nanoparticle formation, but none have unequivocally shown that the resulting nanophase is more stable than the bulk phase. In this paper, we provide clear experimental proof that a thermodynamically stable system containing an inorganic nanophase can be realized through the discovery that a ZnS polytype with a nanosheet morphology is the reaction final state in 17 M NaOH. Our results are consistent with the concept of negative interfacial free energy,[9] but we show that this concept is meaningful only in specific circumstances.

Experimental Section

Nanoparticle Synthesis and Transformation. ZnS nanoparticles (3 nm) were synthesized in water by dropwise addition of 0.01 M Na_2S to 0.01 M $Zn(NO_3)_2 \cdot 6H_2O$ at room temperature. Bulk and nanosheet ZnS were obtained by treating 3 nm nanocrystalline ZnS in NaOH aqueous solution at 230 °C and 2.8 MPa in hydrothermal bombs. After hydrothermal treatment, samples were quenched to room temperature. The solid material was separated by centrifuging and quickly washed with excess ethanol to remove the basic solution without altering the nanosheets.

ZnS is poorly soluble in 17 M NaOH,[18] and we ensured that ZnS was present in excess in each experiment (0.75 g of ZnS in 15 mL of 17 M NaOH). Partial dissolution of the solid ZnS formed a saturated solution, while the remaining ZnS formed nanosheets. In the paper, "17 M NaOH" actually refers to this saturated solution of ZnS in 17 M NaOH. Elemental analyses of the supernatant from bulk ZnS treated for 6 days and 60 days show that the concentrations of Zn^{2+} in the supernatant are the same (0.0156 mol/L), showing that equilibration of ZnS with the solution is achieved in less than 6 days.

The experiment was designed to verify that nanosheet precipitation occurred during the hydrothermal treatment and not during temperature quenching. A temperature gradient was formed within the reaction vessel, and we observed nanosheet formation at a single location. A more uniform distribution of the nanosheet material would be expected if precipitation occurred only during the quenching phase.

X-ray Diffraction. A Rigaku Rint D/max 2500 diffractometer operated in Bragg−Brentano geometry with Cu Kα radiation (λ = 1.5406 Å) was used to identify the crystal structures of initial and coarsened samples. If the full width at half-maximum (fwhm) intensity of each peak is equal to the machine resolution, the sample can be regarded as bulk material.

High-Resolution Transmission Electron Microscopy. HRTEM analyses were performed using a JEOL JEM2010 HRTEM. Samples were prepared for HRTEM study by dispersing ZnS powders onto a holey carbon support.

Results

The experimental framework is shown in Figure 1d. Under most conditions, nanoparticles are thermodynamically metastable with respect to the bulk and will spontaneously grow to form bulk material in the absence of kinetic barriers to coarsening. Accordingly, we find that 3 nm ZnS nanoparticles synthesized in water[18] can be coarsened to form bulk sphalerite ZnS in 0−4 M NaOH under hydrothermal conditions at 230 °C in less than 7 days. The transformation of 3 nm ZnS into bulk ZnS is demonstrated by X-ray diffraction (XRD) (step I, Figure 1a). In contrast, hydrothermal treatment of 3 nm ZnS in an extremely basic solution (17 M NaOH) for over 60 days does not produce bulk ZnS but creates a new phase of nanoscale material (step II, Figure 1a). The XRD data from this material are not consistent with any known zinc oxide, zinc hydroxide, zinc sulfate, or zinc sulfite phase. Furthermore, we also observe that treatment of bulk ZnS under identical conditions also leads to the formation of the same nanoscale material (step III, Figure 1b). Thus the same final state is produced from two different directions (from bulk ZnS and from ZnS nanoparticles), and we believe the final reaction state (i.e., nanosheets in contact with this very basic solution) represents chemical equilibrium and the minimization of the Gibbs free energy of the whole system. The nanosheets can be removed from the reaction vessel, washed, and analyzed, although they are metastable under ambient conditions.

We verified by energy-dispersive X-ray (EDX) fluorescence measurements that the new nanophase is composed purely of Zn and S, with negligible O (Figure 2a, inset). We attribute the small amount of detected O to surface zinc hydroxyl groups, which are known to form on the surface of ZnS nanoparticles synthesized under basic conditions,[20] as well as NaOH not completely removed by the washing steps.[21] Previous work shows that ZnS cannot be oxidized under basic conditions and that hydroxyl groups are not incorporated into the ZnS structure even under extreme hydrothermal conditions, up to 500 atm, 600 °C, and 15 M NaOH.[18,22] Furthermore, after heating this nanophase at 900 °C in a vacuum, XRD gave the typical pattern for pure bulk sphalerite ZnS with no additional phases (step IV, Figure 1a).

Transmission electron microscope (TEM) observations show the nanophase has a sheetlike morphology, with lateral dimension exceeding 600 nm (Figure 2a). Low-magnification images from scanning electron microscopy (SEM) confirm that pure ZnS nanosheets with high homogeneity in their morphology are the sole reaction product (Figure 3 and supplementary Figure S1). Selected area electron diffraction (SAED) patterns reveal individual nanosheets to be single crystals, with an axis of hexagonal symmetry perpendicular to the plane of the sheet (Figure 2a inset). The SAED pattern can be indexed as the [001] zone axis of hexagonal wurtzite-type ZnS crystal. High-resolution TEM images show that the nanosheet phase maintains the close-packed ZnS structure (Figure 2b). Combined with TEM results, the XRD pattern of this nanosheet can be interpreted to represent a superlattice with hexagonal symmetry. The cell parameters of this hexagonal system are a = 3.83 Å, almost the same as standard wurtzite ZnS, and c = 24.14 Å, which is 96.4% of the 4c length in 2H-wurtzite ZnS. A possible packing sequence of nanosheet ZnS along the c axis is {...*ABCABACB*...} or some other close-packed polytype se-

(15) Samia, A. C. S.; Hyzer, K.; Schlueter, J. A.; Qin, C. J.; Jiang, J. S.; Bader, S. D.; Lin, X. M. *J. Am. Chem. Soc.* **2005**, *127*, 4126.
(16) Jun, Y. W.; Lee, J. H.; Choi, J. S.; Cheon, J. *J. Phys. Chem. B* **2005**, *109*, 14795−14806.
(17) Lee, S. M.; Jun, Y. W.; Cho, S. N.; Cheon, J. *J. Am. Chem. Soc.* **2002**, *124*, 11244−11245.
(18) Laudise, R. A.; Ballman, A. A. *J. Phys. Chem.* **1960**, *64*, 688.
(19) Huang, F.; Zhang, H.; Banfield, J. F. *J. Phys. Chem. B* **2003**, *107*, 10470.
(20) Gilbert, B.; Huang, F.; Lin, Z.; Goodell, C.; Zhang, H.; Banfield, J. F. *Nano Letters*, accepted.
(21) Some oxygen can be detected with EDX, between 4 and 9% for different areas of a single crystal of nanosheet, indicating that the O signal is not from within the nanocrystal lattice, but from surface OH absorption incompletely removed by the washing steps.
(22) Scott, S. D.; Barnes, H. L. *Geochim. Cosmochim. Acta* **1972**, *36*, 1275.

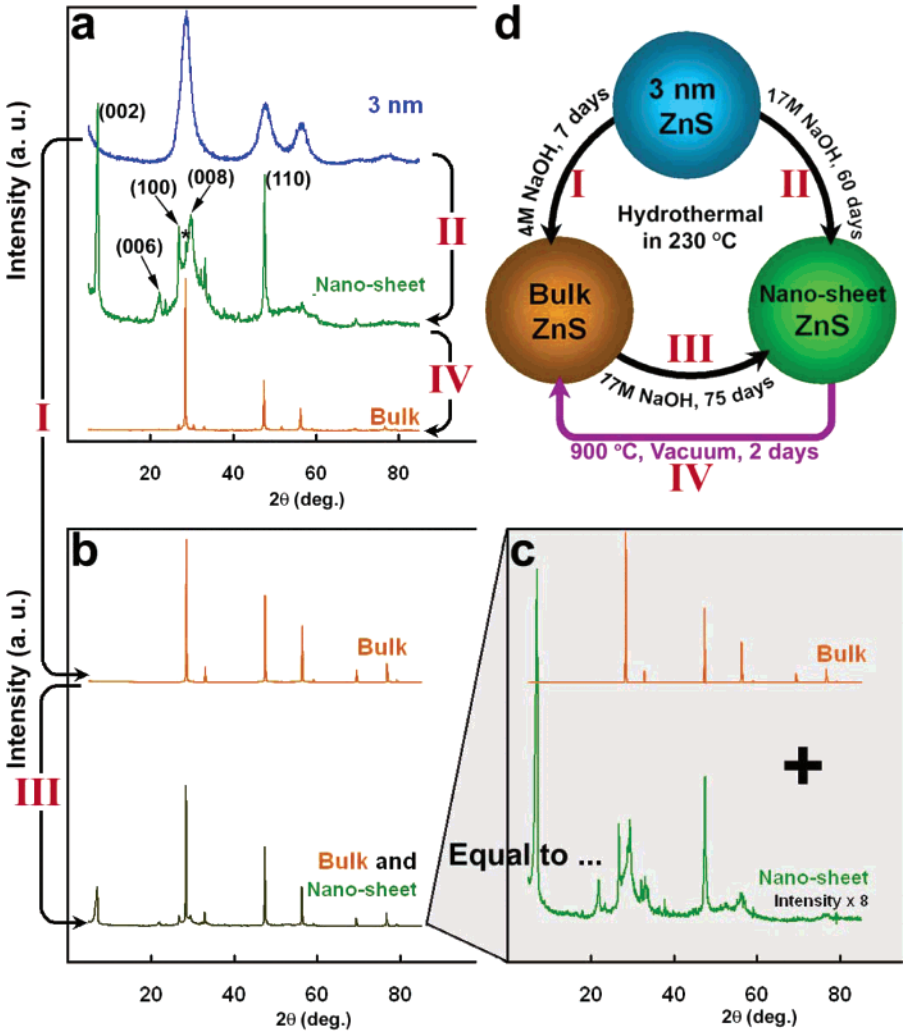

Figure 1. XRD data (a, b, c) and diagram (d) showing the transformation relations among 3 nm ZnS (blue curves), bulk ZnS (orange curves), and nanosheet ZnS (green curves). The XRD data from the new ZnS nanosheet phase is indexed as follows: peak (002) at 7.30° (d = 12.07 Å), (006) at 22.30° (d = 4.02 Å), (100) at 26.95° (d = 3.31 Å), (008) at 29.6° (d = 3.02 Å), (110) at 47.65° (d = 1.908 Å). The peaks at 26.95° and 47.65° fit the (100) and (110) peaks of hexagonal wurtzite ZnS exactly, indicating that the structures of the nanosheet and wurtzite phases are the same in the *ab*-plane. The transformation from bulk to nanosheet ZnS is not complete, as the XRD data obtained from this material (b, black curve) is equivalent to a sum of the patterns from pure bulk ZnS and the nanosheet ZnS given in, as shown in (c).

quence, rather than the standard sequence of wurtzite ZnS, {...*ABAB*...}. For more details see the XRD and wide-angle X-ray scattering (WAXS) analysis in supplementary Figures S2−S4. The Miller indices of the main XRD peaks are shown in Figure 1a. The intensity of the (002) peak is superstrong because the sheetlike morphology leads to a strong effect of preferred orientation in the (001) plane. It is difficult to determine the thickness of the nanosheet through TEM observation. AFM measurements indicate a sheet thickness of approximately 20 nm, consistent with Scherrer analysis of the width of the XRD (002) peak.[23]

Our TEM and XRD measurements show that the nanophase materials obtained by the hydrothermal treatment of ZnS in 17 M NaOH are equivalent whether ZnS nanoparticles or bulk ZnS are chosen as the starting material. In each case, a material with cubic symmetry is transformed into ZnS nanosheets with hexagonal symmetry. The transformation from bulk ZnS is not complete in our samples, but the XRD and TEM data (Figure 1c, d and Figure 2c, d) can be interpreted as a combination of the initial bulk material plus a nanophase material that is structurally and morphologically indistinguishable from the material obtained from the nanoparticle precursor.

(23) Jenkins, R.; Snyder, R. L. *Introduction to X-ray Powder Diffractometry*; John Whiley and Sons: New York, 1996.

Discussion

Our observations are consistent with an effective negative IFE for the close packed ZnS (001) surface. The Gibbs free energy of nanoparticles is the sum of the Gibbs free energy of bulk materials and an interfacial term that is the product of γ, the IFE, and the surface area, A.[5,7]

$$G^{\text{nano}} = G^{\text{bulk}} + \gamma A \qquad (1)$$

At a certain pressure and temperature, a reaction can only spontaneously proceed from a state with higher free energy (metastable phase) to a state with lower free energy (stable phase). Consequently, the experimental results show that ZnS nanosheets with a close-packed (CP) polytype structure have lower molar free energy than bulk sphalerite (Sph) ZnS, i.e., $G_{\text{CP}}^{\text{nano}} < G_{\text{Sph}}^{\text{bulk}}$. Bulk sphalerite ZnS is the stable bulk phase at 230 °C under neutral conditions, and other close-packed ZnS

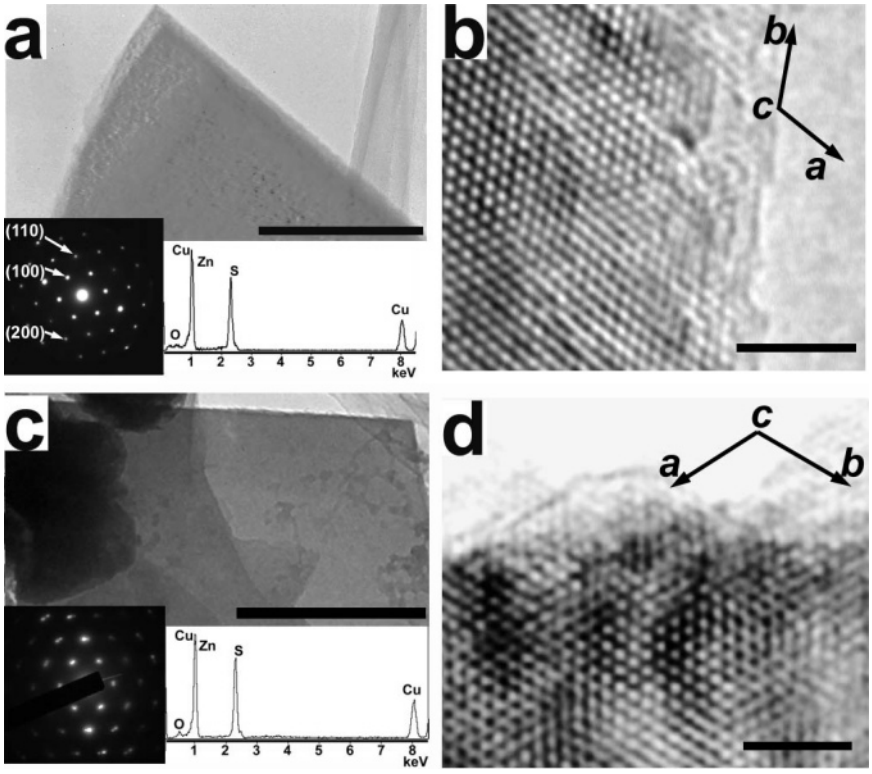

Figure 2. TEM images showing ZnS nanosheets formed at 230 °C in 17 M NaOH. Large scale (a) and high resolution (b) images of sample formed by hydrothermal treatment of 3 nm ZnS for 60 days. Large scale (c) and high resolution (d) images of sample obtained by treating bulk ZnS for 75 days. Image c shows the coexistence of bulk and nanosheet ZnS. Selected area electron diffraction (SAED) and energy-dispersive X-ray (EDX) fluorescence data are given as insets to images a and c. Crystallographic axis directions are indicated on high-resolution images b and d. Scale bar: 150 nm (a), 0.5 μm (c), 3 nm (b, d).

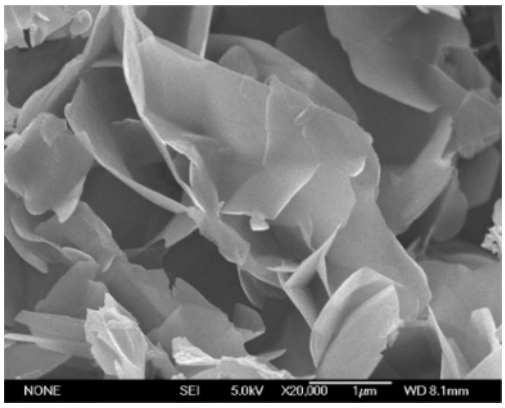

Figure 3. SEM image of an aggregate of ZnS nanosheets, formed by treating ZnS nanoparticles at 230 °C in 17 M NaOH. The thickness of the nanosheets observed in SEM images is consistent with the 20 nm value obtained from X-ray diffraction peak with broadening. Additional SEM images are given in Figure S1.

structures are metastable so $G_{\mathrm{Sph}}^{\mathrm{bulk}} < G_{\mathrm{CP}}^{\mathrm{bulk}}$. The present experimental observations show that

$$G_{\mathrm{CP}}^{\mathrm{nano}} = G_{\mathrm{CP}}^{\mathrm{bulk}} + \gamma A < G_{\mathrm{CP}}^{\mathrm{bulk}} \qquad (2)$$

which implies that $\gamma < 0$.

In general, energetically unfavorable dangling bonds on the surfaces of materials are the reason for the existence of excess positive IFE. According to Gibbs' adsorption law, surface adsorption always acts to lower the IFE from the value for a pristine interface, γ_0. Under conditions of high adsorbate coverage, it has been shown[25] that γ is dominated by the chemical potential of the adsorbate, μ_{ads},

$$\gamma \cong \gamma_0 - (\mu_{\mathrm{ads}} - \mu'_{\mathrm{ads}})\Gamma_{\mathrm{max}} \qquad (3)$$

where μ'_{ads} is defined as the value for which $\gamma = \gamma_0$, and Γ_{max} is the saturated surface adsorbate density. In our system, the chemical potential of the adsorbate can be expressed as[12]

$$\mu_{\mathrm{NaOH,ads}} = \mu_{\mathrm{NaOH,solution}} = \mu_0 + RT \ln(a_{\mathrm{NaOH}}) \qquad (4)$$

Thus, increasing the activity a_{NaOH} leads to an increase in μ_{ads}. In principle, when a_{NaOH} is high enough, $\gamma < 0$ can be achieved. This condition is attainable in microemulsions, and recent density functional theoretical simulations concluded that complete coverage of water in the $\theta-Al_2O_3$ (10-2) surfaces will lead to an effective negative IFE of the whole system ($\theta-Al_2O_3 + H_2O$).[9] The present data are the first experimental demonstration that this effect can drive an inorganic material from bulk to nanoscale dimensions.

Several arguments have been made against the validity of the concept of an effective negative IFE at solid−liquid interface in the presence of strong chemical interactions, and we discuss these in turn. One argument against the formation of a stable material with an effective negative surface energy is the assumption that disintegration of the bulk phase will continue until complete dissolution. However, as shown by earlier descriptions of thermodynamically stable microemulsions,[26]

(24) Zhang, H.; Gilbert, B.; Huang, F.; Banfield, J. F. *Nature* **2003**, *424*, 1025.
(25) Stol, R. J.; De Bruyn, P. L. *J. Colloid Interface Sci.* **1979**, *75*, 185.
(26) Overbeek, J. Th. G. *Faraday Discuss. Chem. Soc.* **1978**, *65*, 7.

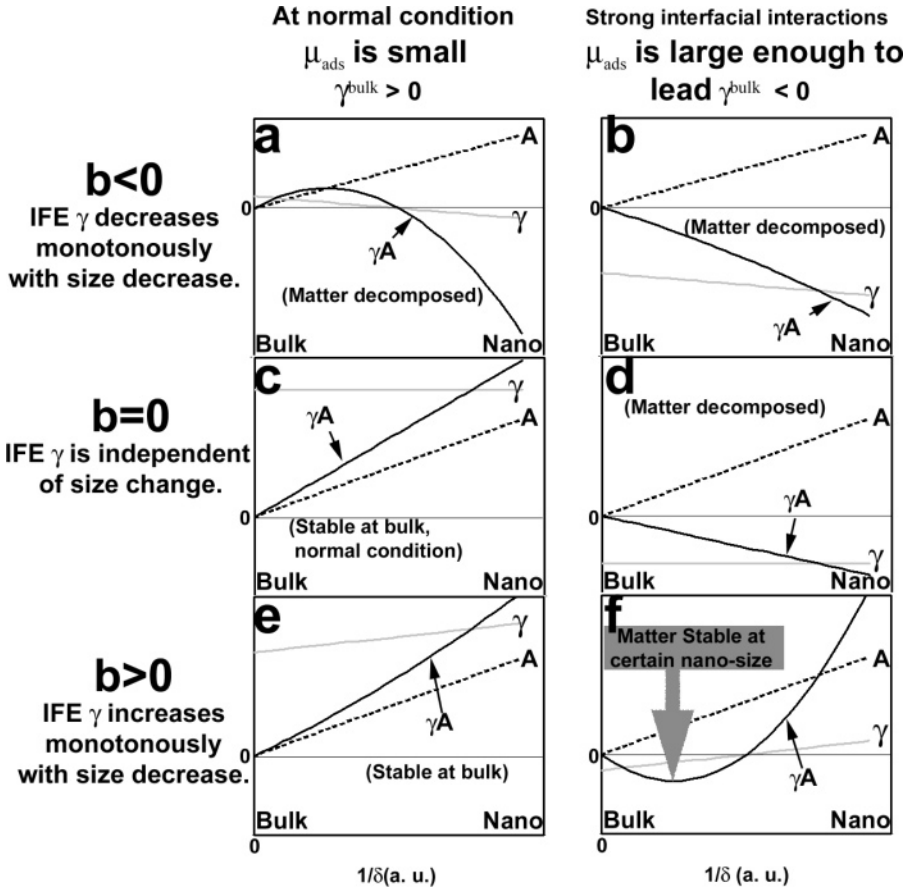

Figure 4. Illustration of the influence of nanosheet thickness (δ) and destabilization coefficient (b) on the thermodynamic parameters γ and γA, under the conditions of low activity ($\gamma^{bulk} > 0$) and high activity ($\gamma^{bulk} < 0$). For $b < 0$, γ decreases monotonically with decreasing particle thickness and γA decreases with the thickness at all concentrations (Figure 4a and b). The solid will disintegrate completely in this situation. For $b \approx 0$, γ is independent of thickness and the bulk phase is thermodynamically stable for most normal conditions (Figure 4c), but in the presence of a very strong surface interaction, γ becomes negative and the material will completely decompose (Figure 4d). Cases a−d are not supported by our experimental observations, while the case $b > 0$ provides a consistent explanation. Under normal conditions ($\gamma^{bulk} > 0$), γA increases with particle thickness, thus the bulk phase is thermodynamically stable (Figure 4e). When strong surface interactions lead to $\gamma^{bulk} < 0$, the size/thickness effect has the tendency to increase γ for small thicknesses. Therefore the product γA (and hence the free energy) has a minimum value at a certain point between bulk and extremely small nanoscale (Figure 4f), where the material is thermodynamically stable.

theoretical treatments of inorganic colloids,[25] and recent DFT simulations,[9] the presence of an additional, size-dependent energetic term in the pristine IFE, γ_0, that contributes more strongly at smaller particle sizes is sufficient to stabilize the system before complete dissolution. A simple thermodynamic model demonstrates that the stability of the ZnS nanosheets involves competition between these terms.

The simplest description of size effect on the IFE is given by

$$\gamma = \gamma_0^{bulk} + b/\delta - (\mu_{ads} - \mu'_{ads})\Gamma_{max} = \gamma^{bulk} + b/\delta \quad (5)$$

where γ_0^{bulk} (γ^{bulk}) is the pristine IFE associate with the surfaces of bulk material without (with) surface adsorption, and δ is the thickness of the nanosheet. The thickness-dependent contribution to γ is the term b/δ, where b is a constant, which is a plausible representation of a destabilizing physical interaction.[27]

Figure 4 illustrates the thermodynamic relationships between bulk and nanoscale phases of a material for different values of the parameters μ_{ads} (adsorption effect) and b (size/thickness effect). Under most scenarios, fine grained ZnS will either coarsen to form bulk ZnS (the normal situation) or disintegrate completely. However, when strong surface interactions lead to $\gamma^{bulk} < 0$, and the size effect has the tendency to increase γ for small thicknesses, the product γA (and hence the free energy) has a minimum value at a certain point between macroscopic and nanoscale dimensions (Figure 4f). At this point, the whole system is thermodynamically stable, and thus nanosheets can be stabilized at a small but finite thickness. We observe that the nanosheet thickness decreases with increasing temperature (Figure S5), supporting our explanation as surface energies normally decrease with temperature,[4] which would cause a lower γ_0 in eq 3.

The anisotropy of crystal structure leads to different numerical values of both pristine interfacial energies and adsorption enthalpies for different termination faces of a material.[29,30] In

(27) In the present system, the nanosheets are stabilized at a thickness around 20 nm (the lateral dimensions are apparently unconstrained). Consequently, we infer the presence of repulsive Coulombic or dipolar electrostatic interactions between the charge distributions at the (001) and (00−1) surfaces. The associated interaction energies have the form b/δ or $\exp(-b\delta)$, respectively, where δ is the nanosheet thickness and b is a positive constant[28]

(28) Israelachvili, J. *Intermolecular and Surface Forces*; Academic Press: San Diego, CA, 2000.
(29) Zhang, H.; Huang, F.; Gilbert, B.; Banfield, J. F. *J. Phys. Chem. B* **2003**, *107*, 13051.
(30) Hamad, S.; Cristol, S.; Catlow, C. R. A. *J. Phys. Chem. B* **2002**, *106*, 11002.

our system, the ZnS (001) face is the dominant surface in the nanosheets. We surmise that crystal faces which exhibit a net excess charge (e.g., ZnS (001)) may permit more complete saturation by adsorption of ions than faces with no excess charge (e.g., ZnS (110), the cleavage face).

A further objection to the concept of an effective negative IFE is the conclusion that it actually indicates that no pure ZnS phase is truly thermodynamically the most stable material. Rather, because the chemical species formed by the interaction of the inorganic surface and the adsorbate is energetically favorable, it represents an attempt to form some other, more stable phase. As the formation of ZnO is not thermodynamically favored for the hydrothermal conditions,[22] the dominant equilibrium is

$$\mathrm{ZnS\ (s) + 4NaOH\ (aq)} \leftrightarrow \mathrm{Na_2ZnO_2\ (s) + Na_2S\ (s) + 2\ H_2O} \quad (6)$$

Crucially, under the experimental conditions, both Na_2ZnO_2 and Na_2S are much more soluble than ZnS. Consequently, the system reaches equilibrium when the solution is saturated relative to the precipitation of ZnS (as nanosheet) but is not saturated relative to the precipitation of any alternative phase of material. Thus, thermodynamic stability is only defined with reference to the system as a whole. Indeed, we emphasize that while the introduction of an effective IFE can create a valid framework to describe the thermodynamic stabilization of inorganic nanoparticles, it is not the only approach available and may be misleading if not presented in a complete form.[31,32]

The resolution of the apparent paradoxes associated with the concept of a negative IFE provides the criteria for the applicability of our method for the synthesis of alternative stable nanophase materials. Additional experiments have shown that CdS nanosheets are not formed with this method, because poorly soluble CdO is thermodynamically favored and rapidly precipitates under all conditions tested. By contrast, as shown in **SOM** Figures S6 and S7, nanoparticles of ZnO are formed when bulk ZnO grains are hydrothermally treated in a suitable solution. Thus, the discovery of thermodynamically stable nanophase materials in contact with an aqueous phase introduces a widely applicable method for synthesizing nanocrystals with control of size and morphology. The particle morphology will be determined by the set of nanocrystal faces that are stabilized, and hence the formation of both nanorods and nanoparticles is feasible with this approach. Semiconductor nanomaterials can be produced on a large scale and without substrate offering novel materials for optoelectronic devices and sensors. Due to the potentially high homogeneity of the product, a combination of growth and self-assembly may permit the formation of ordered 3D nanostructures.

(31) Mathur, A.; Sharma, P.; Cammarata, R. C. *Nature Materials* **2005**, *4*, 186.
(32) Łdziana, Z.; Topsøe, N.-Y.; Nørskov, J. K. *Nature Materials* **2005**, *4*, 186.

Conclusion

We report that by hydrothermal growth of nanocrystalline ZnS under strongly basic conditions, a ZnS polytype with a nanosheet morphology is formed instead of bulk ZnS. Our experiments show the nanosheets to be the equilibrium form of ZnS under the solution conditions, permitting a theoretical description involving an effective negative interfacial free energy. The experimental observation of a material with a formally negative IFE is possible due to thee factors: strong chemical interactions that stabilize one face of the ZnS crystal; a size-dependent destabilizing energetic term that prevents complete disintegration of the nanosheets; and the high solubilities of alternative compounds that prevent their precipitation in place of the ZnS nanosheets.

Acknowledgment. Thanks to an anonymous reviewer for helping with the discussion of the concept of negative IFE. Thanks also transfer to Professor Jillian Banfield and Dr. Hengzhong Zhang at the University of California-Berkeley and to Professor Sishen Xie at the Institute of Physics, Chinese Academy of Science. We thank Feng Bao and Lihua Zhou at the Fujian Institute of Research on the Structure of Matter, Chinese Academy of Sciences for helping with the TEM and SEM. Financial support for this study was provided by the Foundation for Overseas Scholar Fellowship and One Hundred Talent Program in Chinese Academy of Sciences and the National Natural Science Foundation of China (20501021). B.G. was supported by the Director, Office of Science, of the U.S. Department of Energy under Contract No. DE-AC02-05CH11231.

Supporting Information Available: SEM images of ZnS nanosheets; Structural model of ZnS polytype; Analysis of nanosheet structure via the real-space pair distribution obtained from X-ray scattering; Temperature dependence of nanosheet thickness; TEM observations of ZnO nanosheets formed in an equivalent method. Complete ref 20. This material is available free of charge via the Internet at http://pubs.acs.org.

JA057121P

A thermodynamically stable nanophase material

-Supplementary Information

Zhang Lin[1], Benjamin Gilbert[2], Quanlin Liu[3], Guoqiang Ren[1], Feng Huang[1,*]

1. *Fujian Institute of Research on the Structure of Matter, National Engineering Research Center for Optoelectronic Materials, Chinese Academy of Sciences, Fuzhou, Fujian, 350002, People's Republic of China*

2. *Earth Sciences Division, Lawrence Berkeley National Laboratory, Berkeley, CA 94720, U.S. A*

3. *Department of Materials Physics and Chemistry, University of Science and Technology Beijing, Beijing 100083, People's Republic of China*

*Corresponding author: fhuang@fjirsm.ac.cn

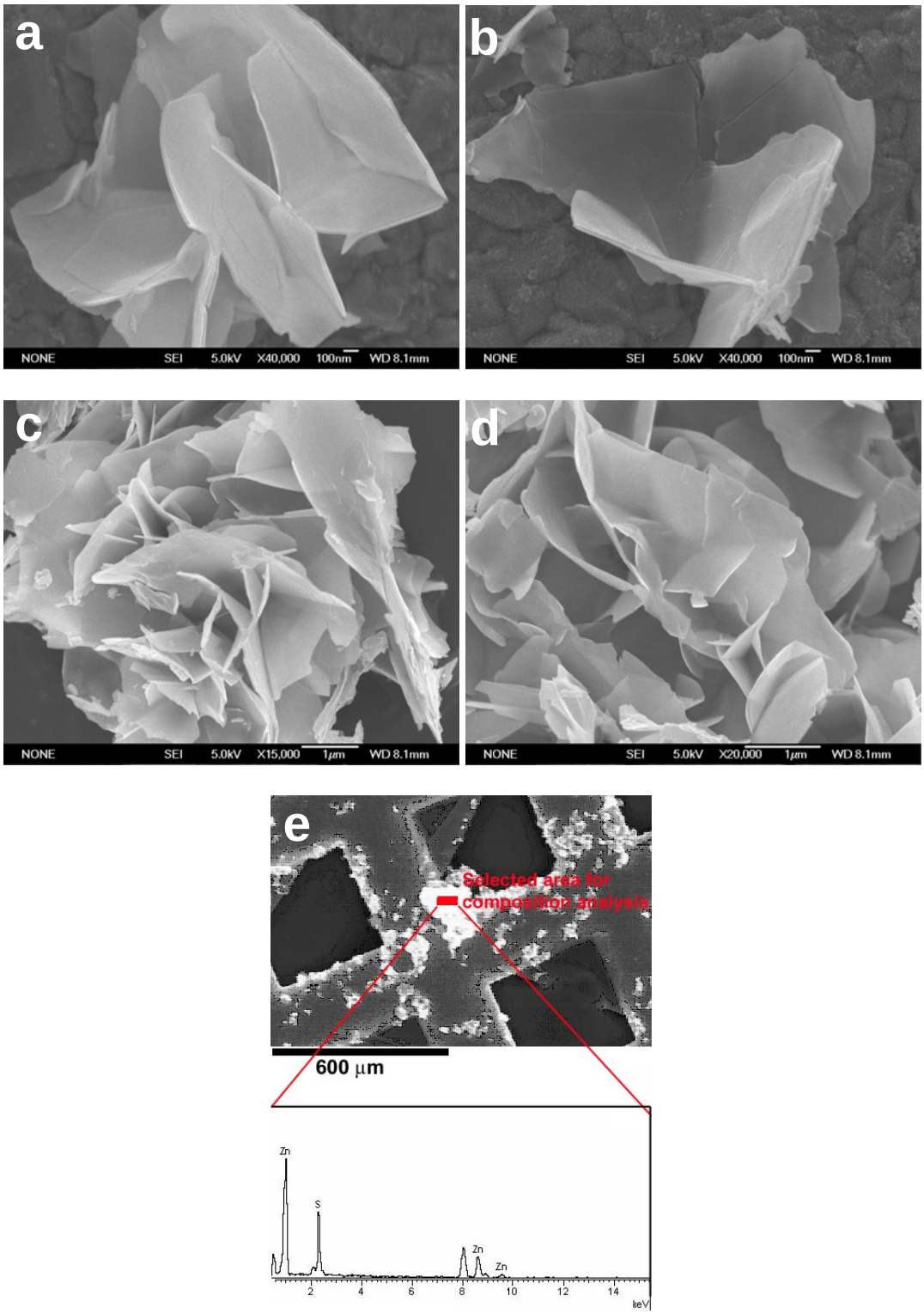

Supplementary Figure S1

Supplementary Figure S1 a),b),c),d) Low-magnification images from SEM showing the homogeneity of the sample in nanosheet morphology. **e)** Selected area element analysis of the nanosheet aggregates showing only Zn, and S elements are present in the sample.

Indexing the nanosheet polytype structure

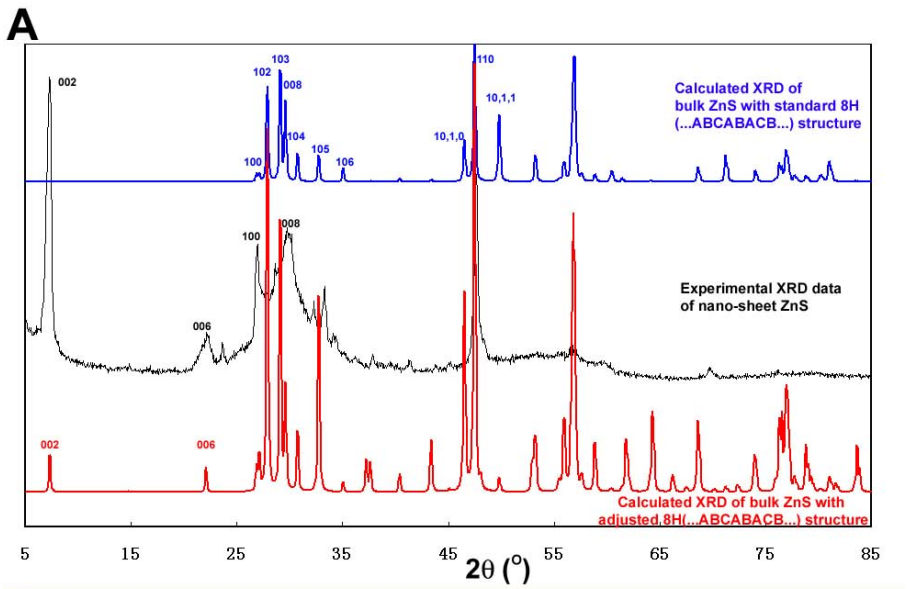

B

#	atom	x	y	z
1	Zn	0.3333	0.6667	1.0000
2	S	0.3333	0.6667	0.0938
3	Zn	0.6667	0.3333	0.1250
4	S	0.6667	0.3333	0.2188
5	Zn	0.0000	0.0000	0.2500
6	S	0.0000	0.0000	0.3438
7	Zn	0.3333	0.6667	0.3750
8	S	0.3333	0.6667	0.4688
9	Zn	0.6667	0.3333	0.5000
10	S	0.6667	0.3333	0.5938
11	Zn	0.3333	0.6667	0.6250
12	S	0.3333	0.6667	0.7188
13	Zn	0.0000	0.0000	0.7500
14	S	0.0000	0.0000	0.8438
15	Zn	0.6667	0.3333	0.8750
16	S	0.6667	0.3333	0.9688

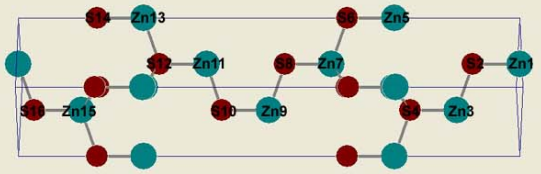

Standarded 8H(...ABCABACB...) Projection plane(110)
Space-group No. 143(P3) *a*=3.83 A, *c*= 24.14A

C

#	atom	x	y	z
1	Zn	0.3333	0.6667	1.0000
2	S	0.3333	0.6667	0.0712
3	Zn	0.6667	0.3333	0.1100
4	S	0.6667	0.3333	0.2088
5	Zn	0.0000	0.0000	0.2600
6	S	0.0000	0.0000	0.3587
7	Zn	0.3333	0.6667	0.3950
8	S	0.3333	0.6667	0.4688
9	Zn	0.6667	0.3333	0.5000
10	S	0.6667	0.3333	0.5713
11	Zn	0.3333	0.6667	0.6100
12	S	0.3333	0.6667	0.7088
13	Zn	0.0000	0.0000	0.7600
14	S	0.0000	0.0000	0.8587
15	Zn	0.6667	0.3333	0.8950
16	S	0.6667	0.3333	0.9688

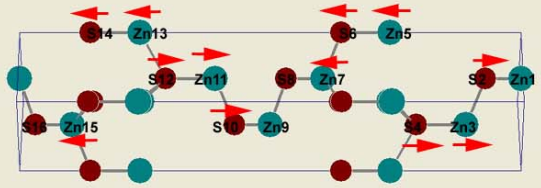

Adjusted 8H(...ABCABACB...) Projection plane (110)
(Arrows: the adjusted directions for atoms in standard 8H)

Supplementary Figure S2 a) Comparison of experimental x-ray diffraction (XRD) pattern from the ZnS nanosheets with the theoretical XRD patterns for bulk ZnS with one wurtzite 8H polytype structure (…*ABCABACB*…), and for bulk ZnS with a modified version of the same 8H polytype. **b) & c)** The atomic positions and unit cell structure of the standard and modified 8H structures. The nanosheet shape and orientation with respect to the crystallographic axes is indicated below.

The indexing of experimental peaks using the standard 8H polytype structure gives fair agreement, except for the presence in the experimental pattern of reflections that are extinct in the standard 8H structure.

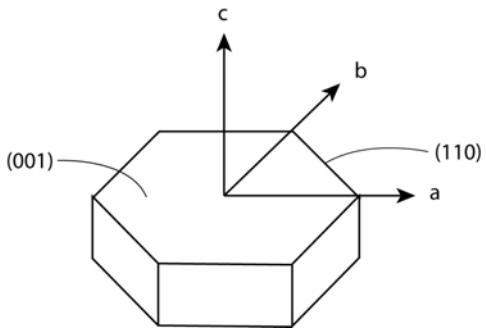

However, while the 8H (002) and (006) peaks are forbidden for the standard 8H structure, these peaks can appear as a result of small adjustments of the atom positions in 8H, and we conclude that the ZnS nanosheet may possess a modified 8H polytype structure. In addition, the nanosheet *c* distance is reduced to 24.14 Å from the standard value of 25.04 Å.

Our structural analysis is incomplete, as the trial modified structure predicts the presence of additional reflections that are not seen in the experimental data: the (103), (104) and (105) peaks. Further analysis will be required to refine the atomic positions in the unit cell, and to incorporate the strong anisotropic shape and preferred orientation effects.

Pair distribution function (PDF) analysis of the nanosheet structure

The structure transformation in ZnS was further studied with synchrotron-based wide angle x-ray scattering (WAXS) measurements to high momentum transfer, from which real-space pair distribution functions (PDF), denoted *G(r)*, were obtained using standard methods [S1, S2]. As shown in Supplementary **Figure S2**, the PDF distinguishes ZnS *cubic-hexagonal* polytypism. The nanosheet PDF is most closely resembles a 8H-wurtzite polytype structure in terms of peak position and intensity, rather than sphalerite or alternative wurtzite 2H, 4H or other 8H polytypes. This result is show in Supplementary **Figure S4**.

Pair distribution functions of bulk ZnS standards.

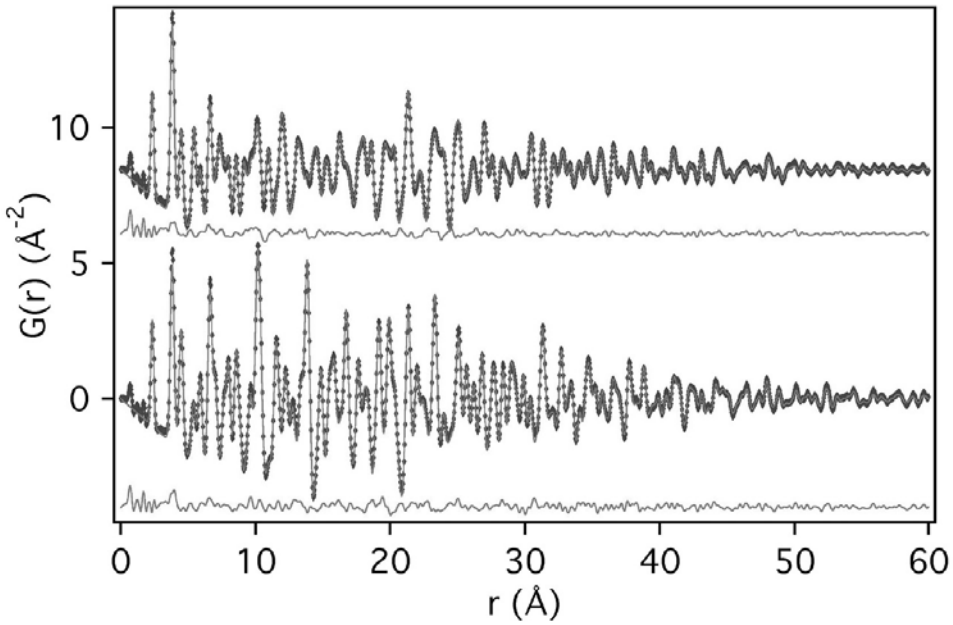

Supplementary Figure S3 Experimental (dots) and simulated (lines) pair distribution functions (PDF) for bulk ZnS with the standard 2H wurtzite (top) and the sphalerite (bottom) structures. As shown by the residuals beneath each curve, the PDF approach is highly quantitative and sensitive to ZnS ***cubic-hexagonal*** polytypism. The decline in PDF peak intensity with increasing interatomic distance, *r*, is an experimental effect of finite angular resolution at the x-ray detector. This effect is constant for all samples.

Experimental vs. simulated PDFs of the nanosheet structure

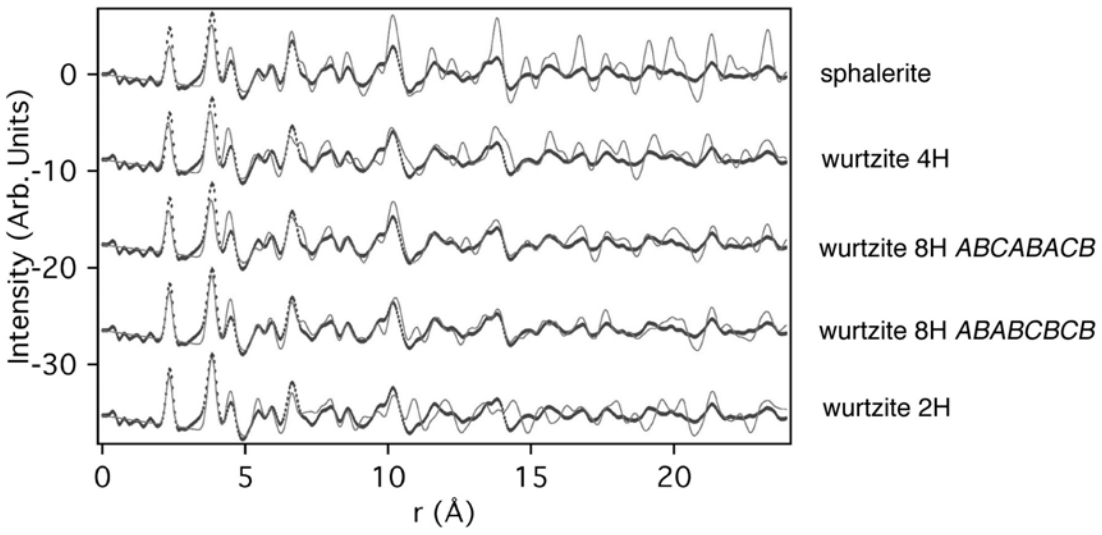

Supplementary Figure S4 Comparisons between the experimental PDF of nanosheet ZnS (dark markers) with simulated PDF patterns for a range of ZnS polytypes (light lines). The wurtzite 8H polytype with the {...*ABCABACB*...} stacking sequence gives the closest match to the experimental data in terms of PDF peak position and intensity. The agreement is not sufficient to conclude that the nanosheet structure contains this particular regular 8H stacking sequence, but indicates that the nanosheet has an associated polytype structure.

[S1] B. J. Thijsse, *J. Appl. Cryst*. **17**, 61 (1984)

[S2] S. J. L., Billinge, M. F.Thorpe (Eds.), *Local Structure from Diffraction* (Plenum, New York, 1998) .

X-ray scattering data were acquired at beamline 11-ID-C of the Advanced Photon Source (APS), and we thank Yang Ren. Use of the APS was supported by the U. S. Department of Energy, Office of Science, Office of Basic Energy Sciences, under Contract No. W-31-109-ENG-38.

Temperature dependence of ZnS nanosheet thickness

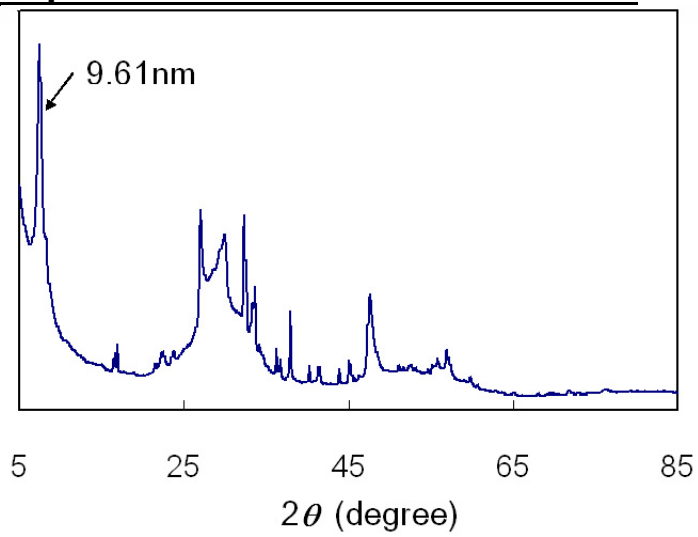

Supplementary Figure S5 X-ray diffraction pattern from ZnS nanosheets synthesized at 250 ˚C. From the width of the (002) peak, the nanosheet thickness calculated with the Scherrer equation is 9.6 nm.

Thermodynamically stable ZnO nanoparticles

Preliminary experiments show that ZnO oxide nanoparticles can be formed at the expense of bulk ZnO under hydrothermal conditions with high surface adsorption.

TEM imaging and diffraction analysis of ZnO nanoparticles

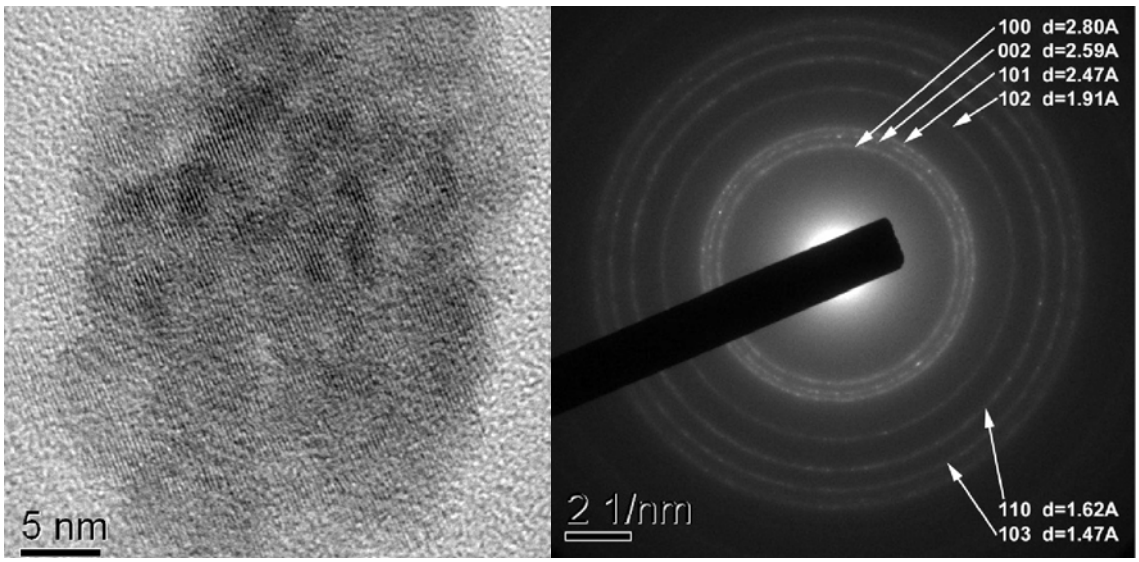

Supplementary Figure S6 Left. Transmission electron microscope image of an aggregate of ZnO nanoparticles formed during the hydrothermal treatment of bulk ZnO. **Right**. Selected area electron diffraction pattern from ZnO nanoparticles. Diffraction rings are indexed in the wurtzite structure, and the broad line width confirms nanoscale particle dimensions.

EDS analysis of ZnO nanoparticles

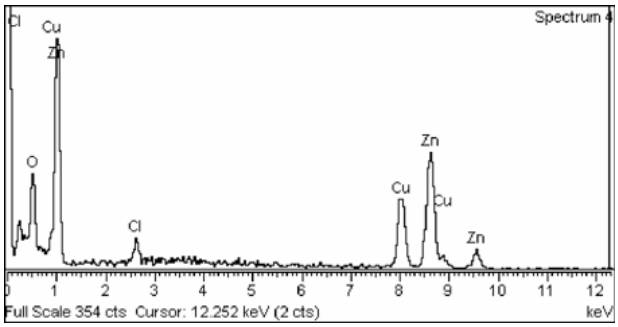

Element	Weight%	Atomic%
O K	5.32	18.25
Cl K	2.12	3.28
Cu K	32.63	28.17
Zn K	59.93	50.30
Totals	100.00	

Supplementary Figure S7 Left. Energy dispersive spectroscopy (EDS) data from ZnO nanoparticles. Copper signal originates from TEM grid. **Right**. Table of elemental composition.